

Temporal Coding in Spiking Neural Networks with Alpha Synaptic Function: Learning with Backpropagation

Iulia M. Comşa^{*1}, Krzysztof Potempa¹, Luca Versari¹, Thomas Fischbacher¹,
Andrea Gesmundo¹, and Jyrki Alakuijala¹

¹Google Research Zürich, Switzerland

January 21, 2022

Abstract

The timing of individual neuronal spikes is essential for biological brains to make fast responses to sensory stimuli. However, conventional artificial neural networks lack the intrinsic temporal coding ability present in biological networks. We propose a spiking neural network model that encodes information in the relative timing of individual spikes. In classification tasks, the output of the network is indicated by the first neuron to spike in the output layer. This temporal coding scheme allows the supervised training of the network with backpropagation, using locally exact derivatives of the postsynaptic spike times with respect to presynaptic spike times. The network operates using a biologically-plausible alpha synaptic transfer function. Additionally, we use trainable synchronisation pulses that provide bias, add flexibility during training and exploit the decay part of the alpha function. We show that such networks can be successfully trained on noisy Boolean logic tasks and on the MNIST dataset encoded in time. We show that the spiking neural network outperforms comparable spiking models on MNIST and achieves similar quality to fully connected conventional networks with the same architecture. The spiking network spontaneously discovers two operating modes, mirroring the accuracy-speed trade-off observed in human decision-making: a highly accurate but slow regime, and a fast but slightly lower-accuracy regime. These results demonstrate the computational power of spiking networks with biological characteristics that encode information in the timing of individual neurons. By studying temporal coding in spiking networks, we aim to create building blocks towards energy-efficient, state-based and more complex biologically-inspired neural architectures.

1 Introduction

Inspired by the biology of the nervous system, artificial neural networks have recently been used to achieve resounding success in solving many real-world problems, sometimes surpassing the performance of humans [1–3]. However, conventional artificial networks lack the intrinsic ability to encode information using temporal coding schemes in the same way as biological brains do. In the nervous system, the timing of individual neuronal spikes is fundamental during behaviours requiring rapid encoding and processing of perceptual stimuli. The relative firing time of neurons has been shown to encode stimulus information in the visual [4], auditory [5] and tactile [6] cortices, but also in higher-level neural structures like the thalamus [7] and hippocampus [8]. Moreover, by observing in-vivo the low latency of responses to visual stimuli in the temporal cortex, it can be concluded that the response is produced by individual spikes occurring at every synaptic stage across the visual areas of the brain [9].

Architectures for atemporal networks that emulate the processing of information in a temporal fashion using memory mechanisms have been proposed [10]. However, these do not have the advantages conferred

^{*}Correspondence: iuliacomsa@google.com

by encoding information in temporal domain. One disadvantage is that every neuron needs to wait for the activation of all the neurons in the previous layer in order to produce an answer. Compared to biological brains, this is inefficient in terms of energy consumption. Moreover, information in the real world almost always has a temporal dimension. Therefore, additional processing is needed for encoding it in an atemporal network, potentially losing information in the process.

Unlike the field of conventional artificial neural networks, the field of artificial spiking networks that encode information in time has not been thoroughly explored. So far, spiking networks have only achieved modest results. The main difficulty in advancing the field of spiking networks has been their training process, as the techniques usually used for supervised learning in atemporal networks cannot be directly applied when information is encoded in a temporal sequence of asynchronous events. Atemporal networks owe much of their success to the development of the backpropagation algorithm [11, 12]. Backpropagation exploits the existence of an end-to-end differentiable relationship between a loss function and the network inputs and outputs, which can be expressed in terms of local derivatives at all hidden network parameters. One can thus find local updates that minimise the loss function and apply them as incremental updates to train the network. On the other hand, in spiking networks, which encode information in sequences of binary spike events, differentiable relationships do not naturally exist.

The problem of training in spiking networks has been addressed in several ways. Many spiking models have adopted a rate coding scheme. In contrast with temporal coding of information, which is based on individual spike timing, rate coding averages over multiple spikes. Approximate gradients have been proposed in order to allow gradient descent optimization in such networks [13–15]. Various other learning rules have been proposed with the objective of producing custom spiking patterns or spike distributions [16–25]. Alternatively, atemporal deep neural networks can be trained and then converted to spiking networks using rate-coding schemes [26–29]. Spiking networks can also be trained using methods such as evolutionary algorithms [30] or reinforcement learning [31]. However, such rate-coding schemes may still be redundant considering the evidence that biological systems can react to stimuli on the basis of single spikes [4, 6, 9].

In contrast with rate-coding models, here we are interested in the temporal encoding of information into single spikes. Crucially, this change in coding scheme shifts the differentiable relationships into the temporal domain. To find a backpropagation scheme for temporal coding, we need a differentiable relationship of the time of a postsynaptic spike with respect to the weights and times of the presynaptic spikes. Encoding information in temporal domain makes this possible.

A similar idea was proposed in the SpikeProp model [32]. In this model, a spiking network successfully learns the supervised XOR problem encoded in temporal domain using neurons that generate single spikes. The model was able to implement backpropagation by approximating the differentiable relationship for small learning rates. It was also necessary to explicitly encode inhibitory and excitatory neurons in order for training to converge. Various extensions to SpikeProp have been proposed [33–36]. Recently, Mostafa [37] trained a spiking network to solve temporally encoded XOR and MNIST problems by deriving locally exact gradients with non-leaky spiking neurons. Other training approaches include spike-timing-dependent plasticity [38] and reinforcement learning [39].

One important choice when modelling a spiking neural network is that of the synaptic transfer function, which defines the dynamics of the neuron membrane potential in response to a presynaptic spike. From a machine learning perspective, this is equivalent to the activation function in conventional networks, but, importantly, it operates in time. Historically, the Hodgkin-Huxley model [40] was the first to offer a detailed description of the process of neuronal spiking using differential equations describing the dynamics of sodium and potassium ionic channels. In practice, however, this model is often needlessly complex. Instead, many applications use the reduced Spike Response Model (SRM) [41]. In this model, the membrane potential is described by the integration of kernels reflecting the incoming currents at the synapse. The neuron spikes when its membrane potential reaches a threshold, then enters a refractory period. Provided that an appropriate kernel function is used [42], the SRM can approximate the dynamics of the Hodgkin-Huxley model to a satisfactory extent, while demanding less computational power and being easier to analyse. Integrate-and-fire neurons and their leaky counterparts are examples of SRM. A commonly used SRM impulse response function is the exponential decay, e^{-t} .

A more biologically-realistic but less explored alternative is the alpha function, of the form te^{-t} , produced by the integration of exponentially decaying kernels. In contrast with the single exponential function, the alpha function gradually rises before slowly decaying (Figure 1a), which allows more intricate interactions between presynaptic inputs. The alpha function has been proposed [43] as a close match to the shape of postsynaptic potentials measured in vitro [44, 45]. It hence provides a biologically-plausible model for exploring the problem-solving abilities of spiking networks with temporal coding schemes. As we show below, it is possible to derive exact gradients with respect to spike times using this model.

With these considerations in mind, here we propose a spiking network model that uses the alpha function for synaptic transfer and encodes information in relative spike times. The network is fully trained in temporal domain using exact gradients over domains where relative spiking order is preserved. To our knowledge, this model has not been previously used for supervised learning with backpropagation. We explore the capacity of this model to learn standard benchmark problems, such as Boolean logic gates and MNIST, encoded in individual spike times. To facilitate transformations of the class boundaries, we use synchronisation pulses, which are neurons that send spikes at input-independent, learned times. The model is easily able to solve temporally-encoded Boolean logic and other benchmark problems. We perform a search for the best set of hyperparameters for this model using evolutionary-neural hybrid agents [46] in order to solve temporally-encoded MNIST. The result improves the state-of-the-art accuracy on non-convolutional spiking networks and is comparable to the performance of atemporal non-convolutional networks. Furthermore, we analyse the behaviour of the spiking network during training and show that it spontaneously displays two operational regimes that reflect a trade-off between speed and accuracy: a slow regime that is slow but very accurate, and a fast regime that is slightly less accurate but makes decisions much faster.

With this work, we also aim to increase the familiarity of the research community with the concept of temporal coding in spiking neural networks. Given that biological brains have evolved for millions of years to use temporal coding mechanisms in order to process information efficiently, we expect that an equivalent development will also be a key step in advancing artificial intelligence in the future. The present work is an early building block in this direction that invites further exploration of more complex recurrent architectures, spike-based state machines and interfacing between artificial and biological spiking neural networks.

2 Methods

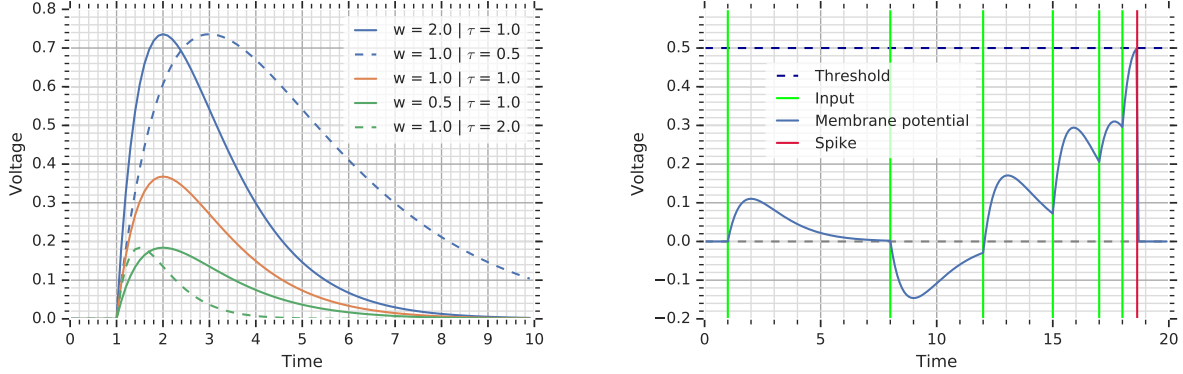
2.1 Temporal coding

In this model, information is encoded in the relative timing of individual spikes. The input features are encoded in temporal domain as the spike times of individual input neurons, with each neuron corresponding to a distinct feature. More salient information about a feature is encoded as an earlier spike in the corresponding neuron. Information propagates through the network in a temporal fashion. Each hidden and output neuron spikes when its membrane potential rises above a fixed threshold. Similarly to the input layer, the output layer of the network encodes a result in the relative timing of output spikes. In other words, the computational process consists of producing a temporal sequence of spikes across the network in a particular order, with the result encoded in the ordering of spikes in the output layer.

We use this model to solve standard classification problems. Given a classification problem with m inputs and n possible classes, the inputs are encoded as the spike times of individual neurons in the input layer and the result is encoded as the index of the neuron that spikes first among the neurons in the output layer. An example drawn from class k is classified correctly if and only if the k^{th} output neuron is the first to spike. An earlier output spike can reflect more confidence of the network in classifying a particular example, as it implies more synaptic efficiency or a smaller number of presynaptic spikes. In a biological setting, the winning neuron could suppress the activity of neighbouring neurons through lateral inhibition [47], while in a machine learning setting the spike times of the non-winning neurons can be useful in indicating alternative predictions of the network. The learning process aims to change the synaptic weights and thus the spike timings in such a way that the target order of spikes is produced.

2.2 Alpha activation function

The neuronal membrane dynamics are governed by a SRM model with alpha function of synaptic transfer [41–43]. This is obtained by integrating over time the incoming exponential synaptic current kernels of the form $\epsilon(t) = \tau^{-1}e^{-\tau t}$, where τ is the decay constant. The potential of the neuronal membrane in response to a single incoming spike is then of the form $u(t) = te^{-\tau t}$. This function has a gradual rise and a slow decay, peaking at $t_{max} = \tau^{-1}$. Every synaptic connection has an efficiency, or a weight. The decay rate has the effect of scaling the induced potential in amplitude and time, while the weight of the synapse has the effect of scaling the amplitude only (Figure 1a).



(a) Alpha potential function with different sets of weights w and decay constants τ . The weight scales the function in amplitude, whereas the decay constant scales it in both amplitude and time.

(b) Example of potential membrane dynamics in response to excitatory and inhibitory inputs, followed by a spike. In this example, $\tau = 1$, $w = \{0.3, -0.4, 0.5, 0.7, 0.5, 0.8\}$, $t = \{1, 8, 12, 15, 17, 18\}$ and the spike occurs at $t_{out} = 18.64$.

Figure 1: Description of the neuron model with alpha synaptic function.

Given a set I of presynaptic inputs i arriving at times $t_i \leq t$ with weights w_i and assuming the postsynaptic neuron has not yet spiked, its membrane potential at time t is given by:

$$V_{mem}(t) = \sum_{i \in I} w_i(t - t_i)e^{\tau(t_i - t)} \quad (1)$$

The neuron spikes when the membrane potential crosses the firing threshold (Figure 1b). To compute the spike time t_{out} of a neuron, we determine the minimal subset of all presynaptic inputs $I_{t_{out}}$ with $t_i \leq t_{out}$ which cause the membrane potential to reach the threshold θ while rising:

$$\sum_{i \in I_{t_{out}}} w_i(t_{out} - t_i)e^{\tau(t_i - t_{out})} = \theta \quad (2)$$

This is achieved by sorting the inputs and adding them to $I_{t_{out}}$ one by one, until an incoming input arrives later than the predicted spike (if any) or there are no more inputs. Note that the set I may not simply be computed as the earliest subset of presynaptic inputs that cause the membrane voltage to cross θ . If a subset of inputs I causes the membrane to cross θ at time t_{out} , any additional inputs that occur between the maximum $t_i \in I$ and t_{out} must be considered, and t_{out} must be recomputed.

Eq. 2 has two potential solutions — one on the rising part of the function and one on the decaying part. If a solution exists (in other words, if the neuron spikes), then its spike time is the earlier of the two solutions.

For a set of inputs I , we denote $A_I = \sum_{i \in I} w_i e^{\tau t_i}$ and $B_I = \sum_{i \in I} w_i e^{\tau t_i} t_i$. The spike time t_{out} can be computed by solving Eq. 2 using the Lambert W function [48, 49]:

$$t_{out} = \frac{B_I}{A_I} - \frac{1}{\tau} W\left(-\tau \frac{\theta}{A_I} e^{\tau \frac{B_I}{A_I}}\right) \quad (3)$$

A spike will occur whenever the Lambert W function has a valid argument and the resulting t_{out} is larger than all input spikes. As we are interested in the earlier solution of this equation, we employ the main branch of the Lambert W function. The Lambert W function is real-valued when its argument is larger than or equal to $-e^{-1}$. It can be proven that this is always the case when Eq. 2 has a solution, by expanding $V_{mem}(t_{max}) \geq \theta$, where $t_{max} = \frac{B}{A} + \frac{1}{\tau}$ is the peak of the membrane potential function corresponding to the presynaptic set of inputs I .

In Appendix A, we show that the proposed model is powerful enough to represent any sufficiently well-behaved function.

2.3 Error backpropagation

The spiking network learns to solve problems whose inputs and solution are encoded in the times of individual input and output spikes. Therefore, the goal is to adjust the output spike times so that their relative order is correct. Given a classification problem with n classes, the neuron corresponding to the correct label should be the earliest to spike. We therefore choose a loss function that minimises the spike time of the target neuron and maximises the spike time of the non-target neurons. Note that this is the opposite of the usual classification setting involving probabilities, where the value corresponding to the correct class is maximised and those corresponding to incorrect classes are minimised. To achieve this, we use the softmax function on the *negative* values of the spike times o_i (which are always positive) in the output layer: $p_j = e^{-o_j} / \sum_{i=1}^n e^{-o_i}$.

We then employ the cross-entropy loss in the usual form: $L(y_i, p_i) = -\sum_{i=1}^n y_i \ln p_i$, where y_i is an element of the one-hot encoded target vector of output spike times. Taking the negative values of the spike times ensures that minimising the cross-entropy loss minimises the spike time of the correct label and maximises the rest.

We minimise the cross-entropy loss by changing the value of the weights across the network. This has the effect of delaying or advancing spike times across the network. For any presynaptic spike arriving at time $t_j \in I$ with weight w_j , we denote $W_I = W(-\frac{\theta}{A_I} e^{\frac{B_I}{A_I}})$ and compute the exact derivative of the postsynaptic spike time with respect to any presynaptic spike time t_j and its weight w_j as:

$$\frac{\partial t_{out}}{\partial t_j} = \frac{w_j e^{t_j} (t_j - \frac{B_I}{A_I} + W_I + 1)}{A_I (1 + W_I)} \quad (4)$$

$$\frac{\partial t_{out}}{\partial w_j} = \frac{e^{t_j} (t_j - \frac{B_I}{A_I} + W_I)}{A_I (1 + W_I)} \quad (5)$$

As the postsynaptic spike time moves earlier or later in time, when $I_{t_{out}}$ changes to include or exclude presynaptic spikes, the landscape of the loss function also changes. Furthermore, the loss function exhibits discontinuities where an output neuron stops spiking; we counter this problem using a penalty, as described below. In practice, we find that optimization is possible in spite of these challenges.

2.4 Synchronisation pulses

In order to adjust the class boundaries in the temporal domain, a temporal form of bias is also needed to adjust spike times, i.e. to delay or advance them in time. In this model, we introduce synchronisation pulses acting as additional inputs across every layer or the network, in order to provide temporal bias across the network. These can be thought of as similar to internally-generated rhythmic activity in biological networks, such as alpha waves in the visual cortex [50] or theta and gamma waves in the hippocampus [51].

A set of pulses can be connected to all neurons in the network, to neurons within individual layers, or to individual neurons. A per-neuron bias is biologically implausible and more computationally demanding, hence in this model we use either a single set of pulses per network, to solve easier problems, or a set of pulses

per layer, to solve more difficult problems. All pulses are fully connected to either all non-input neurons in the network or to all neurons of the non-input layer they are assigned to.

Each pulse spikes at a predefined and trainable time, providing a reference spike delay. Each set of pulses is initialised to spike at times evenly distributed in the interval $(0, 1)$. Subsequently, the spike time of each pulse is learned using Eq. 4, while the weights between pulses and neurons are trained using Eq. 5, in the same way as all other weights in the network.

2.5 Hyperparameters

We trained fully connected feedforward networks with topology `n_hidden` (a vector of hidden layer sizes). We used Adam optimization [52] with mini-batches of size `batch_size` to minimise the cross-entropy loss. The Adam optimizer performed better than stochastic gradient descent. We used different learning rates for the pulse spike time (`learning_rate_pulses`) and the weights of both pulse and non-pulse neurons (`learning_rate`). We used a fixed firing threshold (`fire_threshold`) and decay constant (`decay_constant`).

Network weight initialisation is crucial for the subsequent training of the network. In a spiking network, it is important that the initial weights are large enough to cause at least some of the neurons to spike; in absence of spike events, there will be no gradient to use for learning. We therefore used a modified form of Glorot initialization [53] where the weights are drawn from a normal distribution with standard deviation $\sigma = \sqrt{2.0/(fan_{in} + fan_{out})}$ (as in the original scheme) and custom mean $\mu = \text{multiplier} \times \sigma$. If the multiplication factor of the mean is 0, this is the same as the original Glorot initialization scheme. We set different multiplication factors for pulse (`pulse_init_multiplier`), and non-pulse (`nonpulse_init_multiplier`) weights. This allows the two types of neurons to pre-specialise into inhibitory and excitatory roles. In biological brains, internal oscillations are thought to be generated through inhibitory activities that regulate the excitatory effects of incoming stimuli [54, 55].

Despite careful initialisation, the network might still become quiescent during training. We prevent this problem by adding a fixed small penalty (`penalty_no_spike`) to the derivative of all presynaptic weights of a neuron that has not fired. In practice, after the training phase, some of the neurons will spike too late to matter in the classification and thus they do need to spike at all.

Table 1: Hyperparameters of the model. The first column shows the default parameters chosen to solve Boolean logic problems. The second column shows the search range used in the hyperparameter search. Asterisks (*) mark ranges that were probed according to a logarithmic scale; all others were probed linearly. The last column shows the value chosen from these ranges to solve MNIST.

Parameter	Default value (Boolean tasks)	Search range	Chosen value (MNIST)
<code>batch_size</code>	1	$[1, 1000]^*$	5
<code>clip_derivative</code>	100.0	$[1, 1000]$	539.7
<code>decay_constant</code> (τ)	1.0	$[0.1, 2]$	0.181769
<code>fire_threshold</code> (θ)	1.0	$[0.1, 1.5]$	1.16732
<code>learning_rate</code>	0.001	$[10^{-5}, 1.0]^*$	$10^{-4} \times 2.01864$
<code>learning_rate_pulses</code>	0.001	$[10^{-5}, 1.0]^*$	$10^{-2} \times 5.95375$
<code>n_hidden</code>	1×2	$[0, 4] \times [2, 1000]^*$	1×340
<code>n_pulses</code>	1	$[0, 10]$	10
<code>nonpulse_init_multiplier</code>	0.0	$[-10, 10]$	-0.275419
<code>penalty_no_spike</code>	1.0	$[0, 100]$	48.3748
<code>pulse_init_multiplier</code>	0.0	$[-10, 10]$	7.83912

* - logarithmic search space

Another problem is that the gradients become very large as a spike becomes closer to, but not sufficient for the postsynaptic neuron to reach the firing threshold. In this case, in Eq. 4 and 5, the value of the Lambert W function will approach its minimum (-1) as its argument approaches $-e^{-1}$, the denominator of the derivatives will approach zero and the derivatives will approach infinity. To counter this, we clip the derivatives to a fixed value `clip_derivative`. Note that this behaviour will occur in any activation function that has a maximum (hence, a biologically-plausible shape), is differentiable, and has a continuous derivative.

In addition to these hyperparameters, we explored several other heuristics for the spiking net. These included weight decay, adding random noise during training to the spike times of either the inputs or all non-output neurons in the network, averaging over brightness values in a convolutional-like manner and adding additional input neurons responding to the inverted version of the image, akin to the on/off bipolar cells in the retina. Additionally, to improve the computation time of the network, we tried removing presynaptic neurons from the presynaptic set once their individual contribution to the potential decayed below a decay threshold. This can be achieved by solving an equation similar to Eq. 2 for reaching a decay threshold on the decaying part of the function, using the -1 branch of the Lambert W function. None of these techniques improved our results, so we did not include them here.

2.6 Experiments

2.6.1 Boolean logic problems

We first tested the problem on noisy Boolean logic problems: AND, OR, XOR. For each example, we encoded the two inputs as the individual spike times of the two input neurons. All spikes occurred at times between 0 and 1. We drew True and False values from uniform distributions between $[0.0, 0.45]$ and $[0.55, 1.0]$, respectively. The result is encoded as the first neuron to spike in the output layer. We used a single synchronisation pulse connected to all non-input neurons of the network.

We also solved a concentric circles problem, where the value represents a 2D coordinate uniformly drawn from either an inner circle with a radius of 0.3 or an outer circle with an inner radius of 0.4 and an outer radius of 0.5.

2.6.2 Non-convolutional MNIST

We solved the MNIST benchmark by encoding the raw pixel brightness values in the temporal delay of the 784 neurons of the input layer (Figure 2). All values were encoded as spikes occurring in the interval $(0, 1)$. Darker pixels were encoded as earlier spikes compared to brighter pixels, as they represent more salient information. The scale of the brightness-to-temporal encoding was linear. Input neurons corresponding to white pixels did not spike.

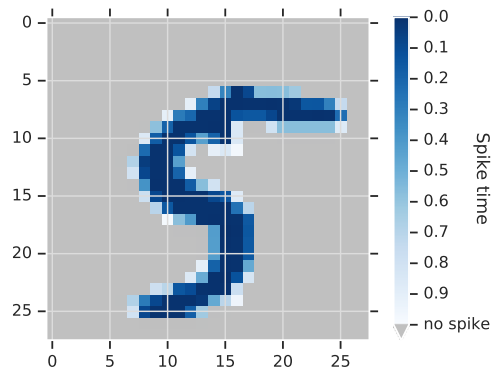


Figure 2: Example of an MNIST digit temporal representation. Each of the 784 input neurons spikes at a time proportional with the brightness of the corresponding pixel in the flattened row-major brightness matrix.

The output of the network was encoded as the first neuron to spike among the 10 neurons in the output layer. We used individual sets of pulses with fixed size connected to each individual layer, in order to allow for deeper architectures where the spike times of different layers might become considerably different.

To find the optimal parameters for solving MNIST, we performed a hyperparameter search using evolutionary-neural hybrid agents [46]. This technique combines deep reinforcement learning with the method of evolutionary agents and has been shown to outperform both approaches in architecture search for a variety of classification tasks. It consists of an evolutionary agent encoding an architecture whose mutations are guided by a neural network trained with reinforcement learning. We used Google Vizier as infrastructure for the hyperparameter search [56].

As detailed in Table 1, the hyperparameter search includes the decay constant of the neurons, whereas the spike times of the inputs are fixed. In this work, we make no claims about the biological meaning of the temporal scales themselves, in particular the spike times of the encoded problem relatively to the decay constant of the model. Rather, we encode well-known problems in time in order to show the general capability of spiking models with temporal coding to solve non-linear, complex problems.

We ran the hyperparameter search with parameter ranges detailed in Table 1. Each trial trained a network on a set of parameters suggested by the hyperparameter search agent within the ranges specified in Table 1. The 60000 MNIST training examples were randomly split into a training set (90%) and a validation set (10%). The final reported objective to be maximised by the search agent was the accuracy on the validation set after 100 epochs. The search was run for 3394 trials. We then chose the hyperparameters of the model as the set that produced the best objective value during the search. These values are given in Table 1.

Finally, we used this set of hyperparameters to train 3 networks for 1000 epochs. This time we trained on the whole MNIST training data with no validation set and tested on the MNIST test data.

2.7 Feature visualisation

We explored the representations learned by the spiking network using the family of “deep dream” methods as commonly applied in atemporal neural networks [57–59]. Given a network with fixed weights and pulses, a blank input image can be gradually adjusted in order to minimise the spike time of a particular neuron. Optionally, at the same time, the spike times of the other neurons in the same layer can be maximised. To do this, a one-hot encoded vector is set as the target for a non-input layer of the network and the derivative with respect to the spike time (Eq. 4) is used to backpropagate errors to the input layer. Then, the same procedure is repeated with the adjusted image, until the output is close enough to the target.

We performed feature visualisation on the network that performed best. We started from a blank image with each pixel initialised to spike at $t = 0.0$, though we confirmed that starting from a random image is also feasible for this procedure. We gradually adjusted the input image once per epoch with a learning rate of 0.1, until the classification produced the correct target class for 10 consecutive epochs. As an additional constraint, we only allowed non-negative spike times.

3 Results

3.1 Boolean logic problems

We first trained small networks containing 2 hidden neurons and 1 synchronisation pulse to solve 2-di-mensional Boolean logic problems encoded in spike times. The networks were trained using the default parameters from Table 1 for a maximum of 100 epochs on 1000 training examples. They were tested on 150 randomly generated test examples from the same distribution. We found that we achieved faster training for these problems when Adam updates were computed and applied only on examples that were classified wrong. In practice, this method has the advantage of discouraging overfitting and reducing the number of operations required for training.

We were able to train such small spiking networks with 100% accuracy on all four problems. Figure 3 exemplifies class boundaries for such networks. All trained networks in these examples had only positive

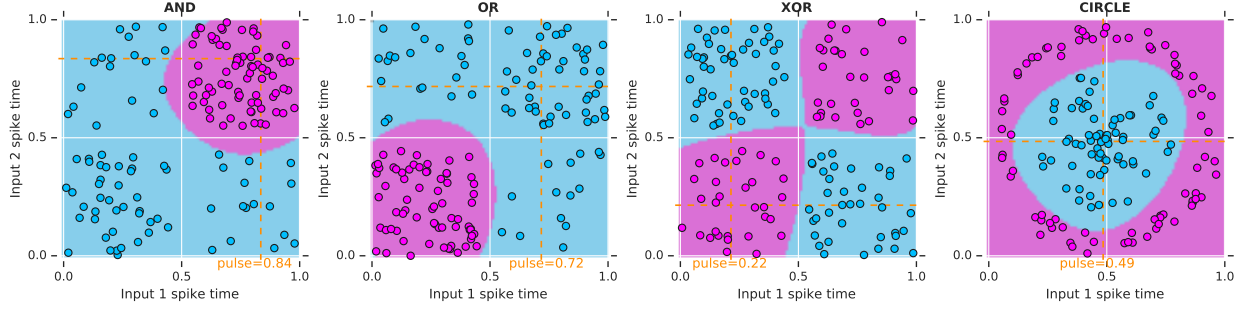


Figure 3: Example of temporal class boundaries produced by small spiking networks with 2 hidden neurons and 1 synchronisation pulse connected to all non-input neurons. All networks are trained for a maximum of 100 epochs on 1000 training examples, while 150 test examples are shown in the figure. The default hyperparameters used for training are shown in Table 1.

weights.

Figure 4 shows the dynamics of the membrane potential of every individual neuron during the classification of a typical XOR example. In this particular case, all neurons spike. With larger spacing between inputs, one of the hidden neurons no longer needs to spike. Given the limited range of inputs with respect to the decay constant, the classification occurs before any significant decay has occurred. However, the network can also be successfully trained with scaled inputs or decay constant so that the time to reach the alpha function peak is exceeded during the classification, in which case the information will also propagate during the decay phase (see Figure 1a).

The purpose of solving a set of simple problems was to demonstrate that spiking networks of a small size can be trained without hyperparameter tuning, and hence we did not focus on performance metrics for these

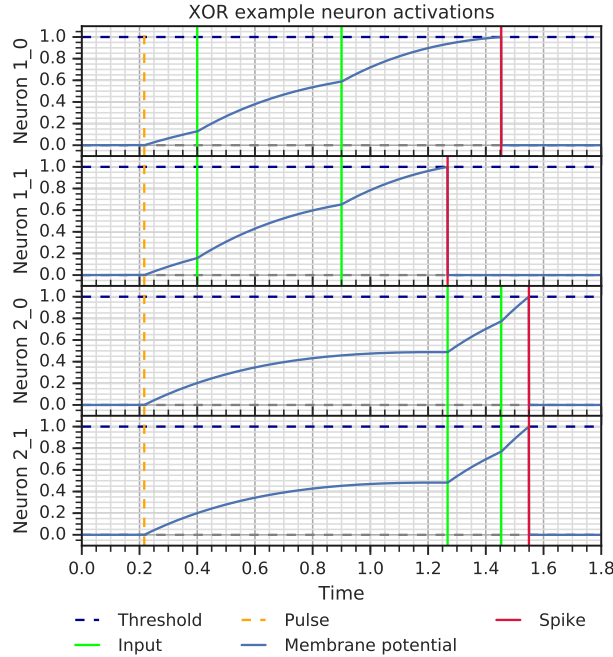


Figure 4: Membrane potentials of hidden (1_*) and output (2_*) neurons during the classification of one XOR example, with incoming inputs at $t = 0.4$ and $t = 0.6$.

problems.

3.2 Non-convolutional MNIST

We found that the best out of the three networks obtained as described in the Methods section reached a maximum accuracy of 99.96% and 97.96% on the MNIST train and test sets, respectively (Table 2). The hyperparameters used to achieve this result are given in Table 1. The hyperparameter values are given in the table up to 6-decimal precision, however in practice an amount of imprecision can be tolerated. In general, the best candidate sets of hyperparameters had a low batch size (up to 5), a small decay rate (between 0.1 and 0.3), and a non-pulse learning rate usually under 10^{-3} , whereas the other hyperparameters had comparatively more varied values.

Table 2: Accuracy of the spiking network trained with the best set of hyperparameters during the slow and fast regimes that occurred spontaneously during training.

	Slow regime	Fast regime
Training accuracy (%)	99.9633	99.885
Training loss (mean)	0.002884	0.00444
Test accuracy (%)	97.96	97.4
Test loss (mean)	0.173248	0.19768

This result improves on recent spiking models published recently (but not trained with conversion from atemporal networks), as detailed in the Discussion. For comparison, we also trained a fully-connected conventional multilayer perceptron with ReLU neurons with the same architecture as the spiking network (784–340–10 neurons) on MNIST. We used the same training setting as for the spiking network: Glorot initialisation, Adam optimizer (learning rate 0.001), the same train/test split, the same number of epochs. We tested batch sizes 5, 32 and 128. For each batch size, we ran the training three times. During the nine runs, we obtained a maximal accuracy of 97.9% on the test set. Although it can be claimed that various techniques can improve the performance of conventional neural networks (as it also may well be the case with the spiking model presented here), we aim to show that, generally-speaking, the performances of the two types of networks are comparable.

During the training process, we observed the same spiking network spontaneously learning two different operating modes for the classification of inputs: a slow regime and a fast regime (Figure 5). In the slow regime, the network spikes in a typical feedforward manner, with the neurons in the output layer usually waiting for all hidden neurons and pulses to spike before spiking themselves. The best accuracy is reported during the slow regime. On the other hand, in the fast regime, the network makes very fast decisions, with the first spike in the output layer occurring before the mean spike in the hidden layer. The transitions between the two regimes is sudden.

Investigating this transition, we found that the input layer pulses had an oscillatory behaviour during training (likely due to a high learning rate pre-set using hyperparameter search) and the transition occurred when these pulses synchronised and simultaneously reached a minimal spike time (0.0). Although they then recovered to larger non-synchronous spike times, this drove the hidden layer pulses to spike considerably earlier (Figure 6). We observed the same transition from a slow to a fast regime occurring in one of the other two trained networks, whereas the third network went directly into a fast regime. With this set of hyperparameters, in particular the relatively high learning rate for pulses leading to oscillatory changes across training epochs, it is likely that the network has a preference for settling into the fast regime.

In the best-performing slow and fast networks, we investigated the individual membrane potentials of the output neurons during the classification of individual examples (Figure 7). We found that all output neurons were first inhibited before producing a spike, even in the case of the fast network. Moreover, in both

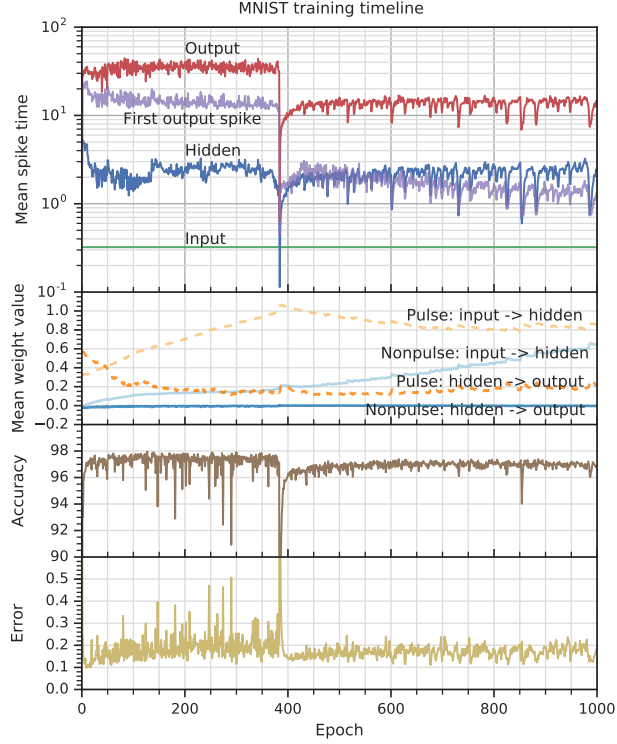


Figure 5: Learning dynamics during the training of a spiking network with the best set of hyperparameters. The plots show a change in regime at epoch 384 from slow to fast classification. All statistics are shown for the test set.

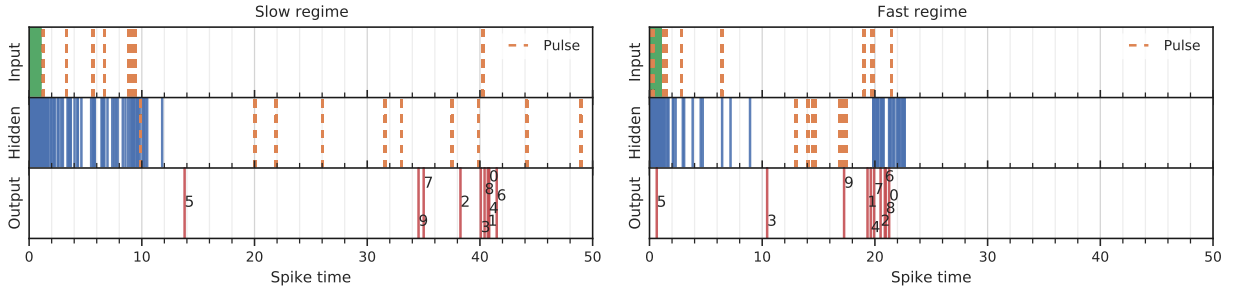


Figure 6: Raster plot of spikes in each layer during the classification of the digit shown in Figure 2 by the best-performing networks with slow and fast regimes. The pulses shown in each layer are connected to the neurons in the next layer. The number labels indicate the digit encoded by an output neuron.

networks, the winning neuron spiked before most or all of the hidden layer pulses spiked. This suggests that one role of the pulses was to produce late spikes where neurons would not have normally spiked, and thus to allow the flow of gradients from non-target neurons during training.

The optimal value for the decay constant (0.181769) chosen by the hyperparameter search means that the alpha function has its maximum at $t = 5.56$. The input spikes were prefixed to occur between 0 and 1. On the other hand, the pulses learned to produce spikes at much later times (Figure 6). This means that the decaying part of the function was exploited indeed, as the output neurons generally spiked only after a subset of the pulses.

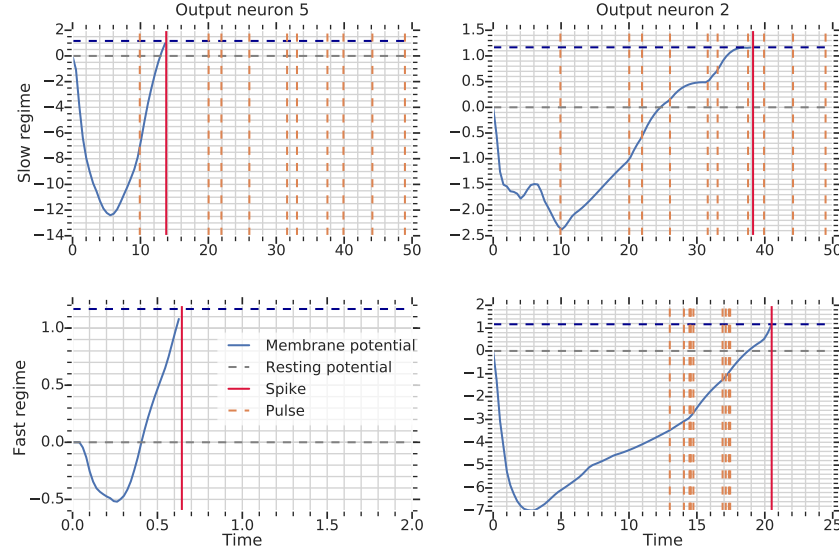


Figure 7: Membrane potentials of two output target and non-target neurons during the classification of the digit shown in Figure 2 by the best-performing networks with slow and fast regimes. The axis scales are different for each plot, reflecting the considerable difference in speed of classification between the two regimes. Inhibition levels (reflected in negative amplitudes) are also considerably different in the two regimes. The membrane potential always becomes hyperpolarised (achieves negative potential) in output neurons before they spike.

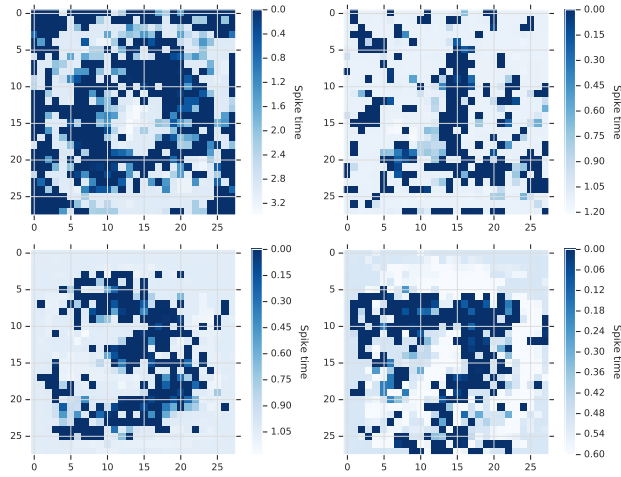


Figure 8: Example of reconstructed input maps that produce a particular output class in the best-performing slow regime network. The target classes are, in row-major order, 0, 1, 3 and 7. The start image is filled with zeros and adjusted using standard gradient descent until the target class is produced 10 epochs in a row. Only non-negative spike times are allowed.

Finally, we investigated whether it was possible to reconstruct target digits using the “deep dream” method. It was indeed possible to produce recognizable digits in this manner (Figure 8).

4 Discussion

In this paper, we proposed a spiking neural network with biologically-plausible alpha synaptic function that encodes information in the relative timing of individual spikes. The activation function is differentiable with respect to time when the presynaptic set is fixed, thus making the network trainable using gradient descent. A set of synchronisation pulses is used to provide bias and extra degrees of freedom during training. We showed that the network is able to successfully solve benchmark problems encoded in time, such as noisy Boolean logic problems and MNIST. Our open-source code and network is openly available at [60].

Our model improves upon existing spiking network models, in particular those from the SpikeProp family, in multiple ways. First, we use a biologically-plausible alpha synaptic function. The alpha function includes a decay component that allows earlier inputs to be forgotten when a neuron has not spiked, which can help in correcting potentially false alarms. We also use a continuous (as opposed to a discretised) scheme where the spike time of an input neuron is proportional to the value of a feature, such as the brightness of a pixel. Finally, we use trainable synchronisation pulses connected to individual layers of the network, which provide temporal bias and allow extra flexibility during training,

Our results on the MNIST benchmark compare favourably with other recent models from literature, including similar models with larger or deeper architectures. Recent works on non-convolutional spiking network whose benchmark results we improve include [28, 37, 61–64]. Recently, performant spiking networks have been obtained by conversion from atemporal neural networks [65], however we are not aware of such networks performing computations by encoding information in the timing of individual spikes.

The main challenge posed by this type of model is the discontinuous nature of the loss function at points where an output neuron stops spiking and due to the landscape changes at the points where the order of pre- and postsynaptic spikes changes. In general, discontinuities also appear in other deep learning models, such as the derivative of the ReLU activation function in atemporal networks. We found that the training process is able to overcome these challenges.

Another practical challenge is the computational complexity of the activation function and the training process. In conventional atemporal networks, the feedforward pass can be performed as a sequence of matrix multiplications, which can be efficiently parallelised on the GPU or other specialised hardware. In spiking networks, the feedforward pass cannot be parallelised in the same efficient fashion, leading to slower training times. In addition, solving the threshold crossing equation in the spiking network requires the computation of exponentials and solving the Lambert W function, which is relatively expensive. The networks presented in this work are trainable on the order of a few seconds to a few hours.

Despite challenges, there are two prominent goals motivating progress in the field of spiking neural networks. On the one hand, spiking neural networks are interesting as computational models of biological processes. They can contribute to understanding low-level information processing occurring in the brain and help us in the search for neural correlates of cognition [66–68]. On the other hand, they can be deployed in neuromorphic hardware [22, 69, 70] to implement rapid and energy-efficient computations.

From a computational biology perspective, the main contribution of this work is showing that it is possible to perform complex, nonlinear computations in networks with biologically-plausible activation functions that encode information in the timing of single spikes. The timing of neuronal spikes, as opposed to spike rates, must play an important role in biological brains during the fast processing of perceptual stimuli. Neurons involved in the processing of sensory stimuli, such as ganglion cells in the retina, fire with very high precision and convey more information through their timing than through their spike count [71]. The relative difference between the first spikes of different ganglion cells can encode the spatial structure of an image [4]. In the primary sensory neurons in human fingertips, the relative timing of the first spikes encodes information about tactile pressure and texture [6]. Further constraints can be inferred from the response times of cortical neurons. In macaque brains, neurons in the temporal area can respond to a visual stimulus within 100ms; given that the anatomy of the visual cortex indicates that at least 10 synaptic stages must be passed to reach the temporal cortex, and given the conduction speed of intracortical fibers and the distance between the brain areas involved, it must be that the response is generated by single, or at most double, spikes in individual neurons [9]. It must therefore be that the temporal encoding of stimuli into single spikes fired by individual neurons are essential in rapid stimulus processing.

More generally, relative spike times are reflected in phase synchronisation between neuronal populations, which can be observed both in individual-neuron studies [5] and in macroscale recording of brain activity [72]. Such synchronisation has been shown to be reliable across different neural stages [5, 7, 8, 73], particularly in dynamic contexts [74]. The relative encoding of information in the precise timing of spikes produced by single neurons is thought to represent a solution to the binding problem — the ability of the brain to coordinate over features highly distributed neural representations, such as associating a colour and a shape with a particular object in the environment [75, 76].

We do not claim that temporal coding is solely responsible for all of the complex cognitive processes performed by biological brains, but rather aim to draw attention that this type of encoding can be an efficient and computationally powerful alternative to rate coding. A reasonable hypothesis is that the two encoding methods are complementary in the brain. A temporal code can be transformed into a rate codes [77] and vice versa [78].

Another point that deserves discussion is backpropagation in biological networks. Our investigation was concerned with the representational capacity, as opposed to the learning mechanism of the network. We therefore used backpropagation to teach the spiking network. The idea of backpropagation in neural networks has for a long time been considered implausible [79], due to requirements such as the existence of symmetrical connections between neuronal layers. However, recent works have begun to challenge this viewpoint and have made promising attempts to understand how backpropagation-like mechanisms might work in a biological network [80–84]. Notably, it has been shown that random feedback connections are able to support learning with backpropagation [83]. The main learning mechanism observed in biological neurons is spike-time dependent plasticity [85], which can theoretically implement weight updates as required by backpropagation [84, 86]. This topic is nevertheless still an open question. Neuroscience is still uncovering the role of neural elements previously thought to have passive roles in the nervous system, which in fact appear to actively participate in synaptic regulation; they might also have significant roles for learning in the brain [87, 88].

To conclude, here we showed that a spiking neural network model with biologically-plausible characteristics is able to solve standard machine learning benchmark problems using temporal coding. These results invite further exploration into the possibility of using such networks to generate behaviours resembling those of biological organisms, as well as investigations into the computational capabilities of spiking neural networks with more complex and recurrent architectures.

On a more speculative note, we expect that further advances in spiking networks with temporal coding will open exciting new possibilities for artificial intelligence, in the same way that it has for biological brains. We envision that neural spike-based state machines will offer a natural solution for the efficient modelling and processing of real-world analogue signals. It will be possible to integrate artificial spiking networks with biological neural networks and create interfaces between the two. These advances will come with significant computing energy savings. By observing and testing models such as the one presented in this study, we aim to increase the familiarity of the research community with the temporal coding paradigm and to create building blocks towards recurrent and state-based architectures for neural computing.

References

- [1] D. Silver, A. Huang, C. J. Maddison, A. Guez, L. Sifre, G. van den Driessche, J. Schrittwieser, I. Antonoglou, V. Panneershelvam, M. Lanctot, S. Dieleman, D. Grewe, J. Nham, N. Kalchbrenner, I. Sutskever, T. Lillicrap, M. Leach, K. Kavukcuoglu, T. Graepel, and D. Hassabis, “Mastering the game of Go with deep neural networks and tree search,” *Nature*, vol. 529, pp. 484–489, jan 2016.
- [2] A. Krizhevsky, I. Sutskever, and G. E. Hinton, “ImageNet classification with deep convolutional neural networks,” *Communications of the ACM*, vol. 60, pp. 84–90, may 2017.
- [3] C. Szegedy, Wei Liu, Yangqing Jia, P. Sermanet, S. Reed, D. Anguelov, D. Erhan, V. Vanhoucke, and A. Rabinovich, “Going deeper with convolutions,” in *2015 IEEE Conference on Computer Vision and Pattern Recognition (CVPR)*, pp. 1–9, IEEE, jun 2015.

- [4] T. Gollisch and M. Meister, “Rapid neural coding in the retina with relative spike latencies,” *Science*, vol. 319, no. 5866, pp. 1108–1111, 2008.
- [5] A. Moiseff and M. Konishi, “Neuronal and behavioral sensitivity to binaural time differences in the owl,” *The Journal of Neuroscience*, vol. 1, pp. 40–48, jan 1981.
- [6] R. S. Johansson and I. Birznieks, “First spikes in ensembles of human tactile afferents code complex spatial fingertip events,” *Nature Neuroscience*, vol. 7, pp. 170–177, feb 2004.
- [7] P. Reinagel and R. C. Reid, “Temporal coding of visual information in the thalamus,” *The Journal of Neuroscience*, vol. 20, pp. 5392–400, jul 2000.
- [8] J. Huxter, N. Burgess, and J. O’Keefe, “Independent rate and temporal coding in hippocampal pyramidal cells,” *Nature*, vol. 425, pp. 828–32, oct 2003.
- [9] S. J. Thorpe and M. Imbert, “Biological constraints on connectionist modelling,” *Connectionism in perspective*, no. July 2016, pp. 1–36, 1989.
- [10] S. Hochreiter and J. Schmidhuber, “Long Short-Term Memory,” *Neural Computation*, vol. 9, pp. 1735–1780, nov 1997.
- [11] B. Speelpenning, *Compiling fast partial derivatives of functions given by algorithms*. PhD thesis, Illinois University, Urbana (USA), 1980.
- [12] D. E. Rumelhart, G. E. Hinton, and R. J. Williams, “Learning Internal Representations by Error Propagation,” tech. rep., US Dept of the Navy, Cambridge, MA, sep 1985.
- [13] Y. Wu, L. Deng, G. Li, J. Zhu, and L. Shi, “Spatio-Temporal Backpropagation for Training High-Performance Spiking Neural Networks,” *Frontiers in Neuroscience*, vol. 12, pp. 1–12, may 2018.
- [14] G. Bellec, D. Salaj, A. Subramoney, R. Legenstein, and W. Maass, “Long short-term memory and learning-to-learn in networks of spiking neurons,” mar 2018.
- [15] C. Lee, S. S. Sarwar, and K. Roy, “Enabling Spike-based Backpropagation in State-of-the-art Deep Neural Network Architectures,” mar 2019.
- [16] D. Sussillo and L. F. Abbott, “Generating coherent patterns of activity from chaotic neural networks,” *Neuron*, vol. 63, pp. 544–57, aug 2009.
- [17] Y. Xu, X. Zeng, L. Han, and J. Yang, “A supervised multi-spike learning algorithm based on gradient descent for spiking neural networks,” *Neural Networks*, vol. 43, pp. 99–113, jul 2013.
- [18] R. V. Florian, “The chronotron: A neuron that learns to fire temporally precise spike patterns,” *PLoS ONE*, vol. 7, no. 8, p. e40233, 2012.
- [19] R. Gütiğ and H. Sompolinsky, “The tempotron: a neuron that learns spike timing–based decisions,” *Nature Neuroscience*, vol. 9, pp. 420–428, mar 2006.
- [20] D. Huh and T. J. Sejnowski, “Gradient Descent for Spiking Neural Networks,” *Advances in Neural Information Processing Systems 31*, pp. 1433–1443, jun 2017.
- [21] F. Zenke and S. Ganguli, “SuperSpike: Supervised Learning in Multilayer Spiking Neural Networks,” *Neural Computation*, vol. 30, pp. 1514–1541, jun 2018.
- [22] E. Neftci, C. Augustine, S. Paul, and G. Detorakis, “Event-driven random backpropagation: Enabling neuromorphic deep learning machines,” in *2017 IEEE International Symposium on Circuits and Systems (ISCAS)*, vol. 11, pp. 1–4, IEEE, may 2017.

- [23] I. Sporea and A. Grüning, “Supervised Learning in Multilayer Spiking Neural Networks,” *Neural Computation*, vol. 25, pp. 473–509, feb 2013.
- [24] S. K. Esser, R. Appuswamy, P. Merolla, J. V. Arthur, and D. S. Modha, “Backpropagation for Energy-Efficient Neuromorphic Computing,” *Neural Information Processing Systems (NIPS)*, pp. 1117–1125, 2015.
- [25] A. Sengupta, Y. Ye, R. Wang, C. Liu, and K. Roy, “Going Deeper in Spiking Neural Networks: VGG and Residual Architectures,” *Frontiers in Neuroscience*, vol. 13, pp. 1–16, mar 2019.
- [26] E. Hunsberger and C. Eliasmith, “Training Spiking Deep Networks for Neuromorphic Hardware,” pp. 1–10, 2016.
- [27] B. Rueckauer and S.-C. Liu, “Conversion of analog to spiking neural networks using sparse temporal coding,” in *IEEE International Symposium on Circuits and Systems (ISCAS)*, vol. 2018-May, pp. 1–5, IEEE, may 2018.
- [28] P. U. Diehl, G. Zarrella, A. Cassidy, B. U. Pedroni, and E. Neftci, “Conversion of artificial recurrent neural networks to spiking neural networks for low-power neuromorphic hardware,” in *IEEE International Conference on Rebooting Computing (ICRC)*, pp. 1–8, IEEE, oct 2016.
- [29] Y. Hu, H. Tang, Y. Wang, and G. Pan, “Spiking Deep Residual Network,” apr 2018.
- [30] N. Pavlidis, O. Tasoulis, V. Plagianakos, G. Nikiforidis, and M. Vrahatis, “Spiking neural network training using evolutionary algorithms,” in *Proceedings. 2005 IEEE International Joint Conference on Neural Networks, 2005.*, vol. 4, pp. 2190–2194, IEEE, 2005.
- [31] R. V. Florian, “Reinforcement learning through modulation of spike-timing-dependent synaptic plasticity,” *Neural Computation*, vol. 19, no. 6, pp. 1468–1502, 2007.
- [32] S. M. Bohte, H. La Poutré, and J. N. Kok, “Error-Backpropagation in Temporally Encoded Networks of Spiking Neurons,” *Neurocomputing*, vol. 48, pp. 17–37, 2000.
- [33] C. Hong, “Training Spiking Neural Networks for Cognitive Tasks: A Versatile Framework Compatible to Various Temporal Codes,” 2017.
- [34] B. Schrauwen and J. Van Campenhout, “Extending SpikeProp,” in *IEEE International Joint Conference on Neural Networks (IEEE Cat. No.04CH37541)*, pp. 471–475, IEEE, 2004.
- [35] S. McKennoch, Dingding Liu, and L. Bushnell, “Fast Modifications of the SpikeProp Algorithm,” in *The 2006 IEEE International Joint Conference on Neural Network Proceedings*, pp. 3970–3977, IEEE, 2006.
- [36] O. Booij and H. tat Nguyen, “A gradient descent rule for spiking neurons emitting multiple spikes,” *Information Processing Letters*, vol. 95, pp. 552–558, sep 2005.
- [37] H. Mostafa, “Supervised Learning Based on Temporal Coding in Spiking Neural Networks,” *IEEE Transactions on Neural Networks and Learning Systems*, pp. 1–9, 2017.
- [38] S. R. Kheradpisheh, M. Ganjtabesh, S. J. Thorpe, and T. Masquelier, “STDP-based spiking deep convolutional neural networks for object recognition,” *Neural Networks*, vol. 99, pp. 56–67, mar 2018.
- [39] M. Mozafari, S. R. Kheradpisheh, T. Masquelier, A. Nowzari-Dalini, and M. Ganjtabesh, “First-Spike-Based Visual Categorization Using Reward-Modulated STDP,” *IEEE Transactions on Neural Networks and Learning Systems*, vol. 29, pp. 6178–6190, dec 2018.
- [40] A. L. Hodgkin and A. F. Huxley, “A quantitative description of membrane current and its application to conduction and excitation in nerve,” *The Journal of physiology*, vol. 117, pp. 500–44, aug 1952.

- [41] W. Gerstner, “Chapter 12. A framework for spiking neuron models: The spike response model,” in *Handbook of Biological Physics*, vol. 4, pp. 469–516, 2001.
- [42] D. Sterratt, B. Graham, A. Gillies, and D. Willshaw, “The synapse,” in *Principles of Computational Modelling in Neuroscience*, pp. 172–195, Cambridge: Cambridge University Press, 2018.
- [43] W. Rall, “Distinguishing theoretical synaptic potentials computed for different soma-dendritic distributions of synaptic input.,” *Journal of Neurophysiology*, vol. 30, pp. 1138–1168, sep 1967.
- [44] K. Frank, “Basic Mechanisms of Synaptic Transmission in the Central Nervous System,” *IRE Transactions on Medical Electronics*, vol. ME-6, pp. 85–88, jun 1959.
- [45] R. E. Burke, “Composite nature of the monosynaptic excitatory postsynaptic potential.,” *Journal of Neurophysiology*, vol. 30, pp. 1114–1137, sep 1967.
- [46] K. Maziarz, M. Tan, A. Khorlin, K.-Y. S. Chang, S. Jastrzębski, Q. de Laroussilhe, and A. Gesmundo, “Evolutionary-Neural Hybrid Agents for Architecture Search,” nov 2018.
- [47] C. Blakemore, R. H. S. Carpenter, and M. A. Georgeson, “Lateral Inhibition between Orientation Detectors in the Human Visual System,” *Nature*, vol. 228, pp. 37–39, oct 1970.
- [48] J. H. Lambert, “Observationes variae in mathesin puram,” *Acta Helvetica*, vol. 3, no. 1, pp. 128–168, 1758.
- [49] R. M. Corless, G. H. Gonnet, D. E. G. Hare, D. J. Jeffrey, and D. E. Knuth, “On the LambertW function,” *Advances in Computational Mathematics*, vol. 5, pp. 329–359, dec 1996.
- [50] W. Klimesch, “Alpha-band oscillations, attention, and controlled access to stored information,” *Trends in Cognitive Sciences*, vol. 16, pp. 606–617, dec 2012.
- [51] G. Buzsaki, *Rhythms of the Brain*. Oxford University Press, 2006.
- [52] D. P. Kingma and J. Ba, “Adam: A Method for Stochastic Optimization,” pp. 1–15, dec 2014.
- [53] X. Glorot and Y. Bengio, “Understanding the Difficulty of Training Deep Feedforward Neural Networks,” in *Proc. of the Int. Conf. on Artificial Intelligence and Statistics*, vol. 9, pp. 249–256, 2010.
- [54] W. Klimesch, P. Sauseng, and S. Hanslmayr, “EEG alpha oscillations: The inhibition–timing hypothesis,” *Brain Research Reviews*, vol. 53, pp. 63–88, jan 2007.
- [55] X.-J. J. Wang and G. Buzsáki, “Gamma Oscillation by Synaptic Inhibition in a Hippocampal Interneuron Network Model,” *The Journal of neuroscience : the official journal of the Society for Neuroscience*, vol. 16, pp. 6402–13, oct 1996.
- [56] D. Golovin, B. Solnik, S. Moitra, G. Kochanski, J. Karro, and D. Sculley, “Google Vizier,” in *Proceedings of the 23rd ACM SIGKDD International Conference on Knowledge Discovery and Data Mining - KDD ’17*, (New York, New York, USA), pp. 1487–1495, ACM Press, 2017.
- [57] D. Erhan, Y. Bengio, A. Courville, and P. Vincent, “Visualizing Higher-Layer Features of a Deep Network,” tech. rep., Département d’informatique et de recherche opérationnelle, 2009.
- [58] A. Mordvintsev, C. Olah, and M. Tyka, “Inceptionism: Going Deeper into Neural Networks,” 2015.
- [59] C. Olah, A. Mordvintsev, and L. Schubert, “Feature visualization,” *Distill*, vol. 2, no. 11, p. e7, 2017.
- [60] “<https://github.com/google/ihmehimmeli>.”
- [61] P. O’Connor and M. Welling, “Deep Spiking Networks,” pp. 1–16, feb 2016.

- [62] A. Tavanaei and A. Maida, “BP-STDP: Approximating backpropagation using spike timing dependent plasticity,” *Neurocomputing*, vol. 330, pp. 39–47, feb 2019.
- [63] D. Querlioz, O. Bichler, P. Dollfus, and C. Gamrat, “Immunity to Device Variations in a Spiking Neural Network With Memristive Nanodevices,” *IEEE Transactions on Nanotechnology*, vol. 12, pp. 288–295, may 2013.
- [64] J. M. Brader, W. Senn, and S. Fusi, “Learning Real-World Stimuli in a Neural Network with Spike-Driven Synaptic Dynamics,” *Neural Computation*, vol. 19, pp. 2881–2912, nov 2007.
- [65] A. Tavanaei, M. Ghodrati, S. R. Kheradpisheh, T. Masquelier, and A. Maida, “Deep learning in spiking neural networks,” *Neural Networks*, vol. 111, pp. 47–63, mar 2019.
- [66] L. M. Ward, “Synchronous neural oscillations and cognitive processes,” *Trends in Cognitive Sciences*, vol. 7, pp. 553–559, dec 2003.
- [67] M. Shanahan, “A spiking neuron model of cortical broadcast and competition,” *Consciousness and Cognition*, vol. 17, pp. 288–303, mar 2008.
- [68] D. Gamez, “Information integration based predictions about the conscious states of a spiking neural network,” *Consciousness and Cognition*, vol. 19, pp. 294–310, mar 2010.
- [69] M. Davies, N. Srinivasa, T.-H. Lin, G. Chinya, Y. Cao, S. H. Choday, G. Dimou, P. Joshi, N. Imam, S. Jain, Y. Liao, C.-K. Lin, A. Lines, R. Liu, D. Mathaikutty, S. McCoy, A. Paul, J. Tse, G. Venkataramanan, Y.-H. Weng, A. Wild, Y. Yang, and H. Wang, “Loihi: A Neuromorphic Manycore Processor with On-Chip Learning,” *IEEE Micro*, vol. 38, pp. 82–99, jan 2018.
- [70] M. Pfeiffer and T. Pfeil, “Deep Learning With Spiking Neurons: Opportunities and Challenges,” *Frontiers in Neuroscience*, vol. 12, oct 2018.
- [71] M. J. Berry, D. K. Warland, and M. Meister, “The structure and precision of retinal spike trains,” *Proceedings of the National Academy of Sciences*, vol. 94, pp. 5411–5416, may 1997.
- [72] S. Palva and J. M. Palva, “The Role of Local and Large-Scale Neuronal Synchronization in Human Cognition,” in *Multimodal Oscillation-based Connectivity Theory*, pp. 51–67, Cham: Springer International Publishing, 2016.
- [73] M. Diesmann, M.-O. Gewaltig, and A. Aertsen, “Stable propagation of synchronous spiking in cortical neural networks,” *Nature*, vol. 402, pp. 529–533, dec 1999.
- [74] R. Lestienne, “Spike timing, synchronization and information processing on the sensory side of the central nervous system,” *Progress in Neurobiology*, vol. 65, pp. 545–591, dec 2001.
- [75] A. K. Engel, P. König, A. K. Kreiter, T. B. Schillen, and W. Singer, “Temporal coding in the visual cortex: new vistas on integration in the nervous system,” *Trends in neurosciences*, vol. 15, pp. 218–26, jun 1992.
- [76] C. M. Gray, “Visual Feature Integration : Still Alive and Well,” *Neuron*, vol. 24, pp. 31–47, 1999.
- [77] E. Ahissar, “Temporal-Code to Rate-Code Conversion by Neuronal Phase-Locked Loops,” *Neural Computation*, vol. 10, pp. 597–650, apr 1998.
- [78] M. R. Mehta, A. K. Lee, and M. A. Wilson, “Role of experience and oscillations in transforming a rate code into a temporal code,” *Nature*, vol. 417, pp. 741–746, jun 2002.
- [79] F. Crick, “The recent excitement about neural networks,” *Nature*, vol. 337, pp. 129–132, jan 1989.

- [80] D. Hassabis, D. Kumaran, C. Summerfield, and M. Botvinick, “Neuroscience-Inspired Artificial Intelligence,” *Neuron*, vol. 95, pp. 245–258, jul 2017.
- [81] Q. Liao, J. Z. Leibo, and T. Poggio, “How Important is Weight Symmetry in Backpropagation?,” pp. 1837–1844, oct 2015.
- [82] Y. Bengio, “How Auto-Encoders Could Provide Credit Assignment in Deep Networks via Target Propagation,” pp. 1–34, jul 2014.
- [83] T. P. Lillicrap, D. Cownden, D. B. Tweed, and C. J. Akerman, “Random synaptic feedback weights support error backpropagation for deep learning,” *Nature Communications*, vol. 7, p. 13276, dec 2016.
- [84] J. C. R. Whittington and R. Bogacz, “An Approximation of the Error Backpropagation Algorithm in a Predictive Coding Network with Local Hebbian Synaptic Plasticity,” *Neural Computation*, vol. 29, pp. 1229–1262, may 2017.
- [85] S. Song, K. D. Miller, and L. F. Abbott, “Competitive Hebbian learning through spike-timing-dependent synaptic plasticity,” *Nature Neuroscience*, vol. 3, pp. 919–926, sep 2000.
- [86] Y. Bengio, D.-H. Lee, J. Bornschein, T. Mesnard, and Z. Lin, “Towards Biologically Plausible Deep Learning,” feb 2015.
- [87] E. A. Newman, “New roles for astrocytes: Regulation of synaptic transmission,” *Trends in Neurosciences*, vol. 26, no. 10, pp. 536–542, 2003.
- [88] C. Eroglu and B. A. Barres, “Regulation of synaptic connectivity by glia,” *Nature*, vol. 468, pp. 223–231, nov 2010.

A Appendix

Here we prove that the proposed spiking network model is an universal approximator for sufficiently well-behaved functions.

Recall that the maximum voltage of a spike of positive weight w is obtained $\frac{1}{\tau}$ units of time after the spike itself, reaching a value of $\frac{w}{\tau e}$.

Lemma 1. *For every $\epsilon > 0$, here is a spiking network with n inputs, each of them constrained to the $[0, 1]$ range, and a single output that produces a spike in the interval $(t, t + \epsilon)$, with $t \geq 2 + \frac{2}{\tau}$ if and only if each of the inputs belongs to a specified interval. Otherwise, no spike is produced. Moreover, it is possible to build one such network by using $2n + 4$ neurons.*

Proof. We will first prove:

Lemma 2. *We can use one neuron and three auxiliary pulse inputs to conditionally produce a spike in the time interval $(t_{out}, t_{out} + \epsilon)$ if and only if the input spike happens at a time t_i that is smaller than (or bigger than) a given constant $t_0 < t_{out}$, provided that $t_{out} > 2 + \frac{1}{\tau}$.*

Proof. Let us consider the function:

$$\Delta_x(t) = w(te^{-\tau t} - (t - T)e^{-\tau t + \tau T}) = we^{-\tau t}(t - (t - T)e^{\tau T})$$

This describes the potential of a neuron that receives one spike at time 0 with positive weight w , and one at time $T \in [-1, 1]$ with negative weight $-w$; note that this formula is valid for $t \geq \max\{0, T\}$. The sign of this function is determined fully by the term $t - (t - T)e^{\tau T}$. Note that $t - (t - T)e^{\tau T} > 0 \Leftrightarrow t(e^{\tau T} - 1) < Te^{\tau T}$.

If $T < 0$, then $e^{\tau T} < 1$, thus $t(e^{\tau T} - 1) < Te^{\tau T} \Leftrightarrow t > -T\frac{e^{\tau T}}{1 - e^{\tau T}}$. As $-T\frac{e^{\tau T}}{1 - e^{\tau T}} < \frac{1}{\tau}$ for $T \in [-1, 0)$, it follows that if $t > \frac{1}{\tau}$ then $\Delta_T(t) > 0$.

If $T > 0$, we have $t(e^{\tau T} - 1) > Te^{\tau T} \Leftrightarrow t > T\frac{e^{\tau T}}{e^{\tau T} - 1}$. As $T\frac{e^{\tau T}}{e^{\tau T} - 1} < 1 + \frac{1}{\tau}$, it follows that if $t > 1 + \frac{1}{\tau}$ then $\Delta_T(t) < 0$.

Thus, we can consider this setup:

- an input spike at time $t_i \in [0, 1]$ with positive weight w ,
- a fixed spike at time $t_0 \in [0, 1]$ with negative weight $w < \theta\tau\epsilon$,
- a fixed spike at time $t_{out} > 2 + \frac{1}{\tau}$ with weight $v \geq \theta\tau\epsilon$,
- a fixed spike at the time when the spike starting at t_{out} would reach the firing threshold if no other spikes were present, with a big enough negative weight to ensure that that spike reaches but does not cross the threshold by itself.

If $t_i \leq t_0$, then at time t_{out} the potential of the neuron is positive (as proven above). Thus, the fixed spike at t_0 will cross the firing threshold and produce an output spike after a small delay (which can be made smaller than ϵ by suitably increasing v). On the other hand, if $t_i > t_0$, the potential will be negative, and no output spike is produced.

In a similar way, we can have a configuration of neurons and weights that will produce a spike in the interval $(t_{out}, t_{out} + \epsilon)$ if and only if $t_i \geq t_0$. \square

By connecting $2n$ of the configurations shown in Lemma 2 to a single neuron, having connections with weight $\frac{\theta\tau\epsilon}{2n-1} - \delta$ for a fixed $\delta > 0$ that depends on the desired ϵ , we obtain an output spike in the interval $(t_{out} + \frac{1}{\tau}, t_{out} + \frac{1}{\tau} + \epsilon)$ if and only if the input belongs to a specified product of intervals. This requires the output spikes of Lemma 2 to belong to an interval that is small enough to ensure that any configuration of input spikes will still reach a potential of θ . This is always possible if the chosen ϵ in Lemma 2 is small enough.

Note that in the configuration from Lemma 2 all the fixed input spikes can be shared, except for the one defining the threshold. Thus, this setup requires at most $2n + 3 + 1$ neurons. \square

Theorem 1. *Let f be a continuous function from $[0, 1]^n$ to $(2 + \frac{2}{\tau}, +\infty)$. Then $\forall \epsilon > 0$, there is a spiking network with 2 hidden layers and decay constant τ that computes a function g satisfying $|f(x) - g(x)| < \epsilon \forall x \in [0, 1]^n$.*

If f is also Lipschitz with constant K , then it is possible to realize such a network using at most $(3K\sqrt{n}\epsilon^{-1})^n(4n + 3) + 1$ neurons.

Proof. Since f is continuous on a compact set, it is uniformly continuous. Thus, for any $\epsilon > 0$, there is a δ such that, in each subdivision of the domain in n -dimensional boxes with extension along each coordinate axis being no more than δ , the difference between the maximum and the minimum of f is at most $\frac{\epsilon}{3}$. Moreover, if the function is Lipschitz with constant K , we can choose $\frac{\epsilon}{3}/(K\sqrt{n})$.

By Lemma 1, for each such box B there is a network that produces a spike in the time interval $(\min_B f, \min_B f + \frac{\epsilon}{3})$ if and only if the input belongs to the box. Connecting the outputs of those networks to a single neuron with sufficiently high weights, we can ensure that it will produce a spike with a delay of at most $\frac{\epsilon}{3}$ after receiving one as an input.

Thus, as a whole the network will produce a spike for input x with a time that is at most ϵ away from the value $f(x)$, proving the thesis. \square

Note that the requirement for the function domain to be greater than some prefixed values is necessary: any network that uses temporal coding, takes two inputs x, y , and produces as an output $\frac{x+y}{2}$ would violate causality.